# A BAYESIAN GEOMETRIC MODEL FOR LINE NETWORK EXTRACTION FROM SATELLITE IMAGES

*C. Lacoste*, X. Descombes, J. Zerubia*

Ariana, joint research group CNRS/INRIA/UNSA,
INRIA, 2004 route des lucioles - BP 93,
06902 Sophia-Antipolis Cedex, France
firstname.lastname@inria.fr

*N. Baghdadi*

BRGM, French Geological Survey
3 avenue Claude-Guillemin - BP 6009,
45060 Orléans, France
n.baghdadi@brgm.fr

## ABSTRACT

This paper presents a two-steps algorithm to perform an unsupervised extraction of line networks from satellite images, within a stochastic geometry framework. First, we propose a new operator providing a measure of the possibility of linear structure presence on each image pixel. Second, we propose a Bayesian model in order to extract the line network from the operator output. The prior model, a Markov object process, incorporates the topological properties of the network through interactions between objects, while the line operator answers are taken into account in the likelihood. Optimization is realized by simulated annealing using a RJMCMC algorithm. An application to hydrographic network extraction is presented.

## 1. INTRODUCTION

Our purpose is to provide an algorithm for line network extraction from satellite images. The final application would be either the production or the update of geographical data. A wide variety of methods have been developed to answer this difficult problem, in particular for the case of road network extraction. One possibility is to consider a semi-automatic approach where an operator gives some checking points [1, 2, 3, 4] in order to initialize a road tracking algorithm. This approach can be extended to a fully-automatic one by an automatic detection of road seeds [5, 6]. Such methods are strongly sensitive to the road seed initialization. In [7], a Markov random field on graph is initialized by a pre-detection of linear features. Here, we propose to perform a pre-processing on the satellite image $I$ providing an output image $Y_I$ where each value measures the possibility of the presence of a line structure on the corresponding pixel of the satellite image. Those values are then considered as noisy data. This is less restrictive than the previous methods because the pre-processing does not initialize some fixed structures or fixed seeds.

*The fi rst author thanks the BRGM for partial funding.

The line network is modeled by a Markov object process, that is to say a random set of objects whose number of points is also a random variable (almost surely finite). The objects of this process are segments described by three random variables corresponding to their midpoint, their length and their orientation. Interactions between segments are taken into account in the prior density $h_p$ of the process, which allows to incorporate constraints on the network topology, such as continuity or slight curvature. Such prior models have been proposed in [8, 9] for road extraction. We choose to take as prior the "Quality Candy" model proposed in [9], which uses quality coefficients for interactions between objects to better model the curvature and the junctions of the network. Contrary to previous works [8, 9] where the likelihood of the observations was replaced by a data term, our approach is Bayesian. Indeed, the likelihood $h_d$ of $Y_I$ given the configuration of segments $S$ can be defined as:

$$h_d(Y_I/S) = h_d(Y_I/X_S)$$

where $X_S$ is a binary image induced by $S$. Our aim is thus to determine the set of segment $S^*$ which maximizes the posterior density defined by:

$$f(S/Y_I) \propto h_p(S)h_d(Y_I/S) \quad (1)$$

Section 2 explains how to obtain the data field $Y_I$. After a recall on the prior density $h_p$ in Section 3, the likelihood $h_d$ is given in Section 4. The optimization - described in Section 5 - is conducted via a simulated annealing. This algorithm is finally tested in Section 6 on a hydrographic network.

## 2. DETECTING LINEAR STRUCTURE PRESENCE

We aim to assign to each pixel of the satellite image a value measuring the possibility of belonging to the line network. To achieve this task, we propose a new operator based on the two usual assumptions made for road extraction:

- $H_1$: *The grey level variation between the structure and the nearby background is large.*
- $H_2$: *The grey level inside the structure is homogeneous.*

For a given number of orientations, we consider a mask of pixels composed of an inside region $V$ (which contains a fixed number of strips) and two collinear regions corresponding to the nearby background. These two regions are positioned at a distance $d$ from $V$ in order to allow a range of widths of the linear structure. An example of a mask is given in Figure 1 for the orientation 0. Let $M_{i,l}$ be the mask

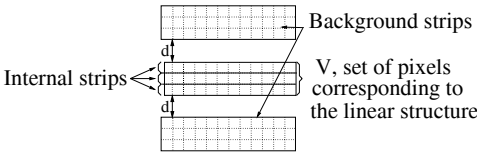


**Fig. 1**. Mask of pixels for the orientation 0.

of orientation $\theta_l$ positioned at pixel $i$. Student's t-tests are used to determine if the averages of the different regions of $M_{i,l}$ are significantly different. $H_1$ and $H_2$ are checked computing respectively $T_{H_1}(i,l)$, the minimum test value between $V$ and the two external regions, and $T_{H_2}(i,l)$, the maximal test value between two internal strips. In order to measure conjointly $H_1$ and $H_2$ for the mask $M_{i,l}$, we compute the following statistical value $t(i,l) = \frac{T_{H_1}(i,l)}{\max\{1\,,\,T_{H_2}(i,l)\}}$. Then, we perform a thresholding of $t(i,l)$ between $t_1$ and $t_2$ and a conversion from $[t_1,t_2]$ to $[0,1]$. For each pixel $j$ belonging to $V(i,l)$, the value $t(i,l)$ is placed in a list of values $L(j)$ associated to $j$. After performing this procedure for each orientation and each pixel, we assign to each $y_k$ of $Y_I$ the maximum of the values contained in $L(k)$. This procedure defines an operator, called "Student Linear Structure Presence" (SLSP) operator. Let note that $y_k$ will be one as soon as a mask containing $k$ strongly supports $H_1$ and $H_2$; it will be zero if any mask containing $k$ does not verify the two hypotheses.

## 3. PRIOR MODEL

The prior model is a Markov object process specified by a density with respect to a uniform Poisson process. The latter corresponds to completely random process (points, lengths and orientations are uniformly and independently distributed) and whose number of points follows a Poisson law. The chosen model, called "Quality Candy" model [9], is based on two relations between segments of the configuration $S$: connection and proximity. Firstly, free segments (not connected) and single segments (connected by only one endpoint) are penalized by a constant positive potential in order to avoid false alarms and to favor line network extension. Secondly, a connection will be more or less favored according to the continuity and the local curvature of the network. Thirdly, all segment pairs verifying the proximity relation are more or less penalized by a positive potential in order to avoid pairs of segments whose midpoints and orientations are too close and to forbid nearby parallel segments (infinite potential in the latter case). So, the prior density can be written as follows:

$$h_p(S) \propto \exp(-U_p(S)) \tag{2}$$

where $U_p(S)$ is the prior energy equal to a weighted sum of potentials computed on the configuration $S$:

$$U_p(S) = \omega_1 n_f + \omega_2 n_s + \omega_3 \sum_{p\in\mathcal{C}} g_c(p) + \omega_4 \sum_{p\in\mathcal{P}} g_p(p)$$

where the $\omega_{i,i=1..4}$ are constant positive weights, $n_f$ (resp. $n_s$) the number of free (resp. single) segments, $\mathcal{C}$ (resp. $\mathcal{P}$) the set of pairs of segments which verify the relation of connection (resp. proximity), and $g_c$ (resp. $g_p$) the potential function corresponding to the connection (resp. the proximity) taking his values in [-1,0] for a connection of good quality and in [0,1] otherwise (resp. taking his values in [0,1]).

## 4. LIKELIHOOD

The output $Y_I$ of the SLSP operator (cf. Section 2) applied to the satellite image $I$, is considered as a noisy data image. The hidden image corresponds to the Boolean image $X_S$ where a pixel takes the value 1 when it belongs to (at least) a mask of pixels associated to a segment of $S$ and 0 otherwise. We suppose that:

$$\mathbf{Y_I} = \mathbf{X_S} + \mathbf{B}$$

where $\mathbf{B}$ is the noise process, defined as follows:

$$B(i) = \begin{cases} |Z(i)| & \text{if} \quad X_S(i) = 0 \\ B(i) = -|Z(i)| & \text{if} \quad X_S(i) = 1 \end{cases}$$

where $\mathbf{Z}$ is a white Gaussian process of variance $\sigma$. The likelihood of $Y_I$ can thus be written as follows:

$$h_d(Y_I/S) = \prod_{j=1}^{N} \underbrace{p(B(j)/X_S(j))}_{2\ p(Z(j))}$$

$$h_d(Y_I/S) = \left(2\sqrt{\frac{\lambda_d}{\pi}}\right)^N \prod_{j=1}^{P} \exp\left(-\lambda_d\,(y_j - X_S(j))^2\right) \tag{3}$$

where $N$ is the number of pixels and $\lambda_d = \frac{1}{2\sigma^2}$.

## 5. OPTIMIZATION

### 5.1. Parameter calibration

The line network minimizing the posterior energy:

$$U(S/Y_I) = U_p(S) + \lambda_d \sum_j (Y_I(j) - X_S(j))^2 \qquad (4)$$

has to verify topological constraints. These constraints can be expressed as constraints on the energy parameters, $\lambda_d$ and $\omega_{i,i=1..4}$.

Firstly, replacing two connected single segments by a free segment - whose mask covers the same pixels as the masks associated with the two single segments - must not induce an energy difference because the hidden image would be the same:

$$2w_2 - w_3 = w_1 \qquad (5)$$

Secondly, we impose that the optimal network does not contain any free segment whose associated mask is composed of less than $n_m$ pixels. That provides:

$$w_1 - \lambda_d \, n_m \geq 0 \qquad (6)$$

Note that equation (6) implies:

$$\lambda_d \, n_m \leq 2 \, w_2 \qquad (7)$$

which implies that the energy decreases when adding a double segment of minimal quality linking two single segments through connections with a negative potential. A segment of minimal quality is defined as a segment which does not verify the proximity relation and whose number of mask pixel values equal to zero is lower than $n_m$.

Thirdly, the optimal segment configuration is not supposed to contain superpositions of segments. This constraint is verified as soon as $\omega_4 > 0$ due to the "hard-core" (infinite) potential imposed on the relation of proximity.

Finally, our segment mask is composed of three strips and we have chosen to take $n_m = 40$ pixels. Taking $\lambda_d = 0.025$, we choose to assign to $w_1$ the lower boundary of values satisfying equation (6): $w_1 = 1$. Choosing $w_2 = 0.7$, we have $w_3 = 0.4$ by equation (5). The chosen positive value for $w_4$ is 1.

### 5.2. MAP Estimation

We aim to find a configuration of segments $S^*$ which maximizes the posterior density $f$:

$$S^* = arg \max_{S \in \bigcup_{n=0}^{\infty} \Omega_n} f(S/Y_I) \qquad (8)$$

where $\Omega_n$ is the set of configurations of $n$ segments and $f$ is given by equation (1). This is a non convex problem for which a direct optimization is not possible given the large size of the state space. We propose to estimate this maximum a posteriori by a simulated annealing embedded in a Reversible Jump Monte Carlo Markov Chain (RJMCMC) algorithm.

The RJMCMC algorithm allows to sample the distribution $\pi$ of a Markov object process specified by an unnormalized density. It consists of simulating a discrete Markov Chain of invariant measure $\pi$ which performs small jumps between the spaces $\Omega_i$ [10, 11]. This iterative algorithm does not depend on the initial state (we consider here the empty configuration). At each step, a transition from the current state to a new state is proposed according to a proposition kernel which is composed of several sub-kernels, each corresponding to a reversible move, such as birth and death of a segment or a symmetrical transformation of segment(s) (ex: rotation). The transition is accepted with a probability given by Green's ratio.

The simulated annealing allows to access to the density modes by performing successive simulations by RJMCMC of processes specified by $f^{1/T}$, with $T$ gradually dropping to 0. Here, we propose to add a decrease temperature schedule on the data weight. Let $\lambda_d(t)$ be the value of this weight at iteration $t$. We start with $\lambda_d(0)$ larger than $\lambda_d$ ($= 0.025$) and perform a slight decrease by plateaus until the iteration $t_f$ such that $\lambda_d(t_f) = \lambda_d$. In this way, a lot of free segment fitting data could be accepted at the beginning of the algorithm as many start points, whereas the constraint of "no free segment" could be respected at the end of the algorithm.

## 6. APPLICATION: RIVER EXTRACTION

This section presents extraction results on a satellite image of Guinea provided by the BRGM (French Geological Survey) shown in Figure 2, where the sought-after cartographic item is a riverine forest. The latter is a hydrographic network, spotted by the presence of trees near rivers. Figure 2 presents the results obtained by our Bayesian approach and by the previous method proposed in [9] (same prior but not used within a Bayesian framework). We have a reference network provided by the BRGM (Fig. 2(c)). A matching of the two networks allow us to compute quantitative criteria of performance, such as $F$, the false alarms ratio, and $O$, the omission ratio, which are given for the two methods in Figure 2. The two extracted line networks are continuous with few omissions and false alarms in spite of the low image contrast and the line network sinuosity. Working within a Bayesian framework definitely improves the performances (no omission, no break, low overdetection ratio). Moreover, the computing time is reduced due to the use of a pre-computing for the likelihood (which is possible thanks to the SLSP operator) and the simple hypotheses we have made on noise: $Y_I$ was obtained in 1 minutes, (d) in 4 min-

(a) Satellite image I (b) $Y_I$ (b) Reference (d) $F \sim 0\%$ - $O \sim 11\%$ (e) $F \sim 10\%$ - $O \sim 14\%$

**Fig. 2**. Results of line network extraction from a satellite image - (a) original image ($682 \times 674$ pixels, resolution: 20 m) - (b) output of the SLSP operator - (c) reference line network, manually extracted by an expert (BRGM) - (d) extraction with our Bayesian model (e) extraction with "Quality Candy" model with a data term instead of the likelihood.

utes and (e) in 20 minutes with a processor of 2 GHz.

## 7. CONCLUSION

We have proposed in this paper a relevant method to perform unsupervised line network extraction from satellite image. The use of the SLSP operator based on statistical tests seems to be adapted to the construction of data for our Bayesian Markov object model. The Maximum A Posteriori estimation provides a continuous, smooth extracted line network with low omission and overdetection ratios, improving the results of [9]. The adding of a decrease schedule on the data weight allows to accept a lot of free segments well-positioned in the first iterations of the simulated annealing and thus to arise algorithm performance. A parameter tuning rule has been defined from geometrical constraints allowing to easily fix the density parameters. Taking into account these constraints, we will focus in a near future on the estimation of density parameters. Moreover, the proposed stochastic modeling allows us to consider working in a frame of data fusion in order to benefit from the contribution of several sources (for instance, outputs provided by different operators or multi-sensor data). Finally, this modeling could be extended to more complex objects such as broken lines which would adapt themselves more easily to sinuous networks.

## 8. REFERENCES


[1] M. A. Fischler, J. M. Tenenbaum, and H. C. Wolf, "Detection of roads and linear structures in low-resolution aerial imagery using a multisource knowledge integration technique," *Computer Graphics and Image Processing*, vol. 15, pp. 201–223, 1981.

[2] D. Geman and B. Jedynak, "An active testing model for tracking roads in satellite images," *IEEE Trans. on PAMI*, vol. 18, pp. 1–14, 1996.

[3] N. Merlet and J. Zerubia, "New prospects in line detection by dynamic programming," *IEEE Trans. on PAMI*, vol. 18, no. 4, pp. 426–431, 1996.

[4] W. M. Neuenschwander, P. Fua, L. Iverson, G. Székely, and O. Kubler, "Ziplock snakes," *International Journal of Computer Vision*, vol. 25, no. 3, pp. 191–201, 1997.

[5] M. Barzohar and D. B. Cooper, "Automatic finding of main roads in aerial images by using geometric-stochastic models and estimation," *IEEE Trans. on PAMI*, vol. 18 - 2, pp. 707–721, 1996.

[6] A. Zlotnick and P. Carnine, "Finding road seeds in aerial images," *Computer Vision, Graphics, and Image Processing*, vol. 57, pp. 243–260, 1993.

[7] F. Tupin, H. Maitre, J-F. Mangin, J-M. Nicolas, and E. Pechersky, "Detection of linear features in SAR images: Application to road network extraction," *IEEE Trans. on Geoscience and Remote Sensing*, vol. 36, no. 2, pp. 434–453, 1998.

[8] R. Stoica, X. Descombes, and J. Zerubia, "A Gibbs point process for road extraction in remotely sensed images," To appear in International Journal of Computer Vision.

[9] C. Lacoste, X. Descombes, and J. Zerubia, "Road network extraction in remote sensing by a Markov object process," in *ICIP*, Barcelona, Spain, Sept. 2003.

[10] C. J. Geyer and J. Møller, "Simulation and likelihood inference for spatial point process," *Scandinavian Journal of Statistics, Series B*, vol. 21, pp. 359–373, 1994.

[11] P.J. Green, "Reversible jump Markov chain Monte-Carlo computation and Bayesian model determination," *Biometrika*, vol. 57, pp. 97–109, 1995.